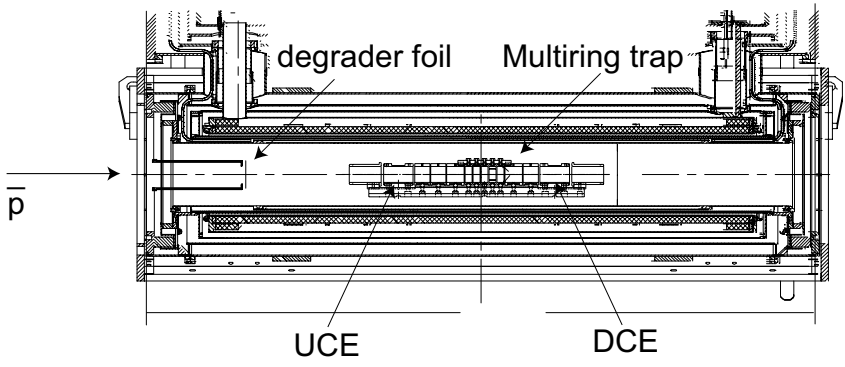

Figure 3: ASACUSA trap design. Multiring trap were placed inside the superconducting solenoid. The vacuum isolation foils are also shown.

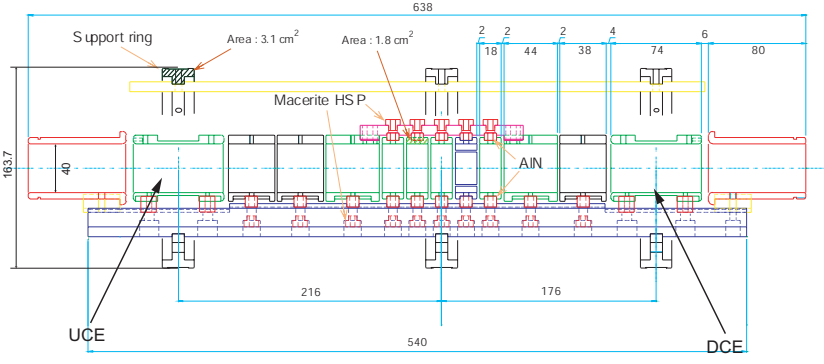

Figure 4: Configuration of the MRT electrodes.

at around the MRT. The ramping speed of the magnetic field was 0.03 T/s. The size of the solenoid was 1.42 m in length and 22 cm in inner diameter. The inner diameter of the UHV bore tube in which the MRT was housed was 165 mm. Both ends of the bore tube were supported by eight motor controlled linear feedthrough rods (four rods on each side), which enabled precise alignment of the bore tube axis with respect to the solenoid axis. Adjustment of ± 2 mm is possible on both ends in 1 μm steps with stepping motors. The cryostat had the capability to cool the bore tube down to 2.2 K by pumping one end of the liquid helium cooling loop covering all over the bore tube. To supply a large amount of liquid helium, the reservoir had a volume of 330 l.

The MRT was adopted for the trapping and cooling of antiprotons because of its large catching volume and higher stability, which are necessary to handle a large number of charged particles while keeping the space-charge effects relatively small [12]. The ring

electrodes had 40 mm in diameter. The lengths of electrodes were 18 mm, 38 mm, 44 mm, 74 m, and 80 mm, each other (Fig. 4). A set of electrodes, UCE and DCE (in Fig. 4), were used to catch injected antiprotons by applying high voltages. Central 5 ring electrodes provided a harmonic potential where nonneutral plasmas were stably confined as rigid spheroids [12]. Charged particles were confined axially by this electrostatic field by the ring electrodes and radially by the magnetic field of the superconducting solenoid.

In our experiments, the solenoid and the MRT were operated under conditions as followings;

- the strength of the magnetic field was 2.5 T,
- the temperature of the bore tube was $\leq$ 5 K,
- the catching potential applied to the UCE and DCE was -10 kV,
- and the depth of the harmonic potential was 50 V.

Before the antiproton incidence, electrons were injected from a field emission array cathode from the downstream side of the MRT where no foils located. The emitter was on a pneumatic type feedthrough which was retracted during the extraction procedure of ultra-slow beams to avoid intercepting extracted antiproton beams. The typical number of stored electrons was 3×10^8. They formed a pure electron plasma. In the 2.5 T strong magnetic field, electrons lose their energy continuously by synchrotron radiation and cooled to nearly down to the ambient temperature. The captured antiprotons cooled via collisions with the electrons. This electron plasma cooled the newly arrived antiprotons continuously. The energy which electrons received from the antiprotons was dissipated spontaneously by synchrotron radiation with a time constant of about 1 s [7, 13].

These electron cooling processes were observed by exciting axially symmetric electrostatic oscillation of the joint plasma by applying white noise to it via one of the trap electrodes [14]. These oscillations induced peaks in the power spectrum at the corresponding mode frequencies, and the shift of these peaks with time was used to monitor the antiprotons cooling process. The cooling time was experimentally obtained, which was about 30 s for 10 keV antiprotons [14].

2.2 Transport beam line

The main purpose of the transport beam line was a differential pumping between the MRT region and a collision chamber with 10^{-6} mbar where a gas target was used. This feature was realized by using three sets of electrostatic lenses consisting of size-variable and electrically floatable apertures installed in the beam line (VA1, VA2 and VA3 in Fig. 5) [15]. These apertures separated the beam line into 4 rooms; the room directly connected to the MRT, where a tandem turbo molecular pumps (250 liter and 70 liter turbo pumps) was used, the second room was pumped by a 1000 liter and 70 liter turbo pumps (TMP1 in Fig 5), the third was 400 liter turbo pump (TMP2), and the final room was connected to the collision chamber.

Trajectory calculations were performed for antiprotons starting from the trap region under influences of both magnetic and electrostatic forces by using finite element method [15].

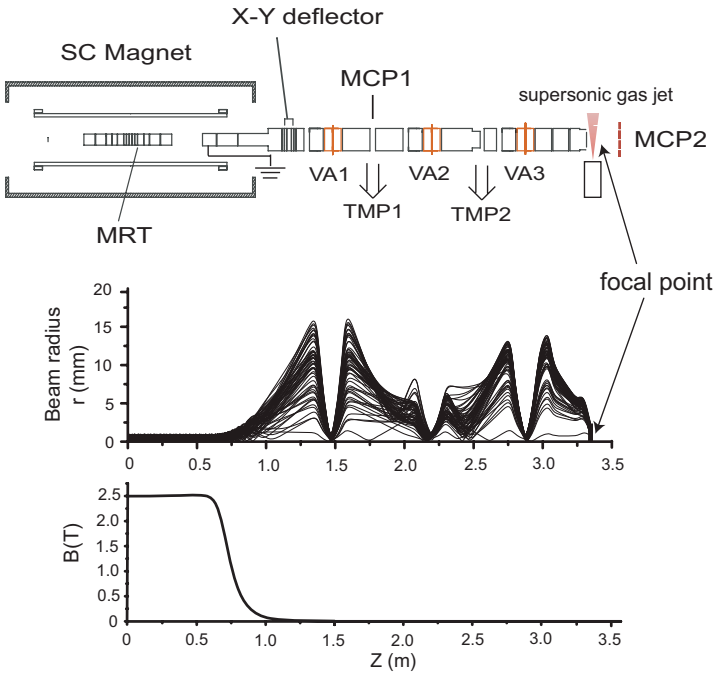

Figure 5: Design of the transport beam line. Calculated trajectories of antiprotons and the strength of the magnetic field by the superconducting solenoid are also shown.

The calculated trajectories of antiprotons show that the antiproton cloud whose radius is 1 mm with energies of 1 eV in the perpendicular direction relative to the magnetic field can be effectively extracted without any loss, although charged particles follow the magnetic field line and diverge. The results are shown in Fig. 5.

The extraction energy was tunable from 10 to 500 eV by floating whole electrodes of the transport beam line.

3 Experimental results

3.1 Track detector

For diagnostic purposes it was important to know the position and time distribution of antiproton annihilations during the capture, storage, and cooling of antiprotons. Annihilation detectors consisting of two 2 m long plastic scintillator bars were used for this purpose. They were placed parallel to the trap axis, at distances of 40 and 74 cm from

it, and had cross sections of 4(H) × 6(V) cm^2, thus subtending overlapping solid angles of 0.12 sr seen from the center of MRT trap axis. Coincident pulse produced in a scintillator by the passage of a charged particle from antiproton annihilation were detected by photomultiplier tubes at the ends of the bar. Their arrival-time differences corresponded to the hit position of the particle. The annihilation position was evaluated as the intersection of the trap axis and the line connecting hit positions of each bars with a precision of $\sim$ 50 mm in FWHM. We performed particle-tracking simulations using the GEANT library [16], from which we estimated the overall detection efficiency to be $\sim$ 5% at the center of the trapping region.

3.2 Antiproton confinement

The trapping, cooling, and extraction procedure of antiprotons is shown in Fig. 6:

(a) The antiprotons pulse proceeded along the MRT axis to the position of the last (downstream) electrode (DCE in Fig. 6), which being biased at -10 kV reflected it to the upstream ring, UCE. Before the first antiprotons in the pulse passed through the UCE, the trap was closed around the pulse by a MOS-FET switch which changed the bias of the UCE to -10 kV. By this time, most of the 90 ns long pulse had entered the trap. From the result of measurements using track detector, it was found that antiprotons were lost at the positions of the trap and the vacuum isolation foil, although about half of the captured antiprotons remained in the MRT after a few seconds.

(b) Within 30 s almost all antiprotons were cooled via collisions with the preloaded electrons, and captured in the harmonic potential region. Annihilation rate fell down. As described in Sec.2.1, the antiproton cooling process was non-destructively monitored by observing electrostatic modes of the electron plasma.

(c) The preloaded electrons were removed from the trapping region by opening and closing the trap for 550 ns several times after the cooling. This is because considerable amount of antiprotons were lost during the slow extraction when the electrons were kept [14].

(d) For efficient extraction of ultra-slow antiprotons, antiprotons were gathered around the axis of the trap by utilizing radial compression technique [17].

(e) Then by gradually ramping up the trapping potential antiprotons were extracted out of the field free region.

The captured antiprotons of 1.2×10^6 could be stably stored in the MRT for periods of 10 min or more, although they were usually ejected earlier. This number of stored antiprotons is typically more than 50 times higher than the previous best values obtained with relatively thick degrader foils [8]. With a 30% RFQD transmission efficiency for the decelerated particles and the aforementioned 70% efficiency of transmission through the PET foils, the overall antiproton trapping efficiency, defined as the number captured versus the number in the AD shot, was 4%. By stacking five AD shots in sequence [8], 5×10^6 antiprotons, the largest number of antiprotons ever stored and cooled, were confined in our MRT.

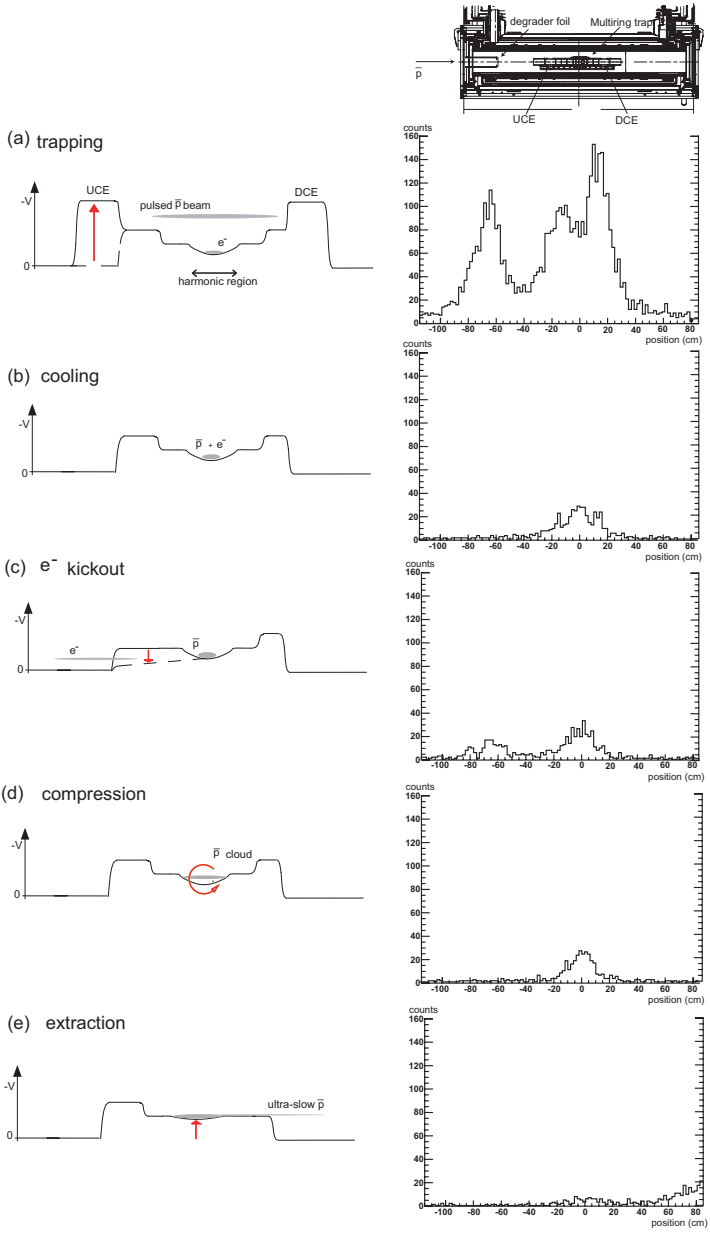

Figure 6: Antiproton trapping, cooling, and extraction procedure. Annihilation counts were integrated over 15 s for each procedures.

Table 1: Summary table of antiproton trapping and extraction efficiency of MUSASHI.

	energy	
$\bar{p}$ production	2.8 GeV	4×10^7/AD shot
AD	5.3 MeV	2×10^7/AD shot
RFQD	110 keV	>25%
degrader	$\leq$ 10 keV	∼70%
MRT	$\leq$ 1 eV	30-50%

3.3 Extraction of antiprotons as ultra-slow beams

Finally antiprotons were extracted from the trapping region by gradually ramping up the potential. The extraction continued over a period of $\sim$ 10 s. These cooled antiprotons were extracted at 250 eV. We also tested the extraction at 10, 100, and 500 eV in energy. The transport efficiency did not vary against any extraction energy.

For confinement and cooling of antiprotons, our MUSASHI worked every AD shots, *i.e.*, every 84 s, but for extraction of ultra-slow antiprotons beams it took more than 3 AD shots. For efficient extraction, it took more than 100 s for radial compression of trapped antiproton cloud.

4 Summary

We developed the ultra-slow antiproton beam source, MUSASHI, composed of the antiproton trap and ultra-slow beam transport line. As many as 1.2×10^6 cooled antiprotons were accumulated per AD shot; this is at least 50 times larger than the best value reported with thick-foil energy degrader method. The cold antiprotons of 250 eV was then extracted out of the strong magnetic field after the radial compression. The efficiency of MUSASHI for production of ultra-slow antiproton beams was summarized in the Tab. 1.

This work was supported by the Grant-in-Aid for Creative Scientific Research (10P0101) of the Japanese Ministry of Education, Culture, Sports and Technology (MonbuKagakushō), Special Research Projects for Basic Science of RIKEN, and the Hungarian National Science Foundation (OTKA T033079).

References

[1] Y. Yamazaki, Nucl. Instru. Methods B 154 174 (1999).
[2] H. Knudsen and J.F. Reading, Phys. Rep. 212 352 (1994).
[3] A. Trzińska *et al.*, Phys. Rev. Lett. 87 082501 (2001).
[4] M. Wada *et al.*, in Non-Neutral Plasma Physics IV, edited by F. Anderegg *et al.*, AIP Conf. Proc. No. 606 (AIP, New York, 2001), p.625.
[5] G. Gabrielse *et al.*, Phys. Rev. Lett. 57 2504 (1986).
[6] M.H. Holtzscheiter *et al.*, Phys. Lett. A 214 279 (1996).

[7] G. Gabrielse *et al.*, Phys. Rev. Lett. 63 1360 (1989).
[8] G. Gabrielse *et al.*, Phys. Lett. 548B 140 (2002).
[9] A.M. Lombardi, W. Pirkl, and Y. Bylinsky, in proceedings of the 2001 Particle Accelerator Conference, Chicago (IEEE, Piscataway, 2001), p.585.
[10] M. Hori *et al.*, Phys. Rev. Lett. 91 123401 (2003).
[11] H.A. Torii *et al.*, to be submitted.
[12] A. Mohri *et al.*, Jpn. J. Appl. Phys. 37 664 (1998).
[13] B.R. Beck, J. Fajans, and J. Malmberg, Phys. Plasmas 3 1250 (1996).
[14] N. Kuroda *et al.*, Phys. Rev. Lett. 94 023401 (2005).
[15] K. Yoshiki Franzen *et al.*, Rev. Sci. Instrum. 74 3305 (2003).
[16] CERN Application Software Group, GEANT version 3.21.
[17] N. Kuroda *et al.*, to be submitted.